The Netherlands Press

Journal of Airline Operations and Aviation Management

Article

PITCH MOVEMENT AND ANALYSIS OF AIRCRAFT USING OPENVSP

[*1]Sajaratuddur, [2]Lelya Hilda

[1]Faculty of Chemical Engineering,
Universitas Islam Negeri Sumatera Utara, India

Orchid ID: https://orcid.org/0000-0002-4820-8631

Email: sajaratuddur@uinsu.ac.id

[2]Faculty of Chemical Engineering,
Institute Agama Islam Negeri Padangsidimpuan, INDONESIA,

Orchid ID: https://orcid.org/0000-0002-0607-1761

Email: lelyahilda@iain-psp.ac.id

Abstract.

There are many different design options available thanks to the growing number of customised solutions in the aircraft design process, which mostly rely on new technology at the component level. In addition, there is a rising need for a uniform, intelligible data model due to the process' increased complexity as well as the increasing number of possible fixed-wing aircraft configurations. Design is made simpler by the use of parametric geometry tools like Vehicle Sketch Pad (OpenVSP), which express geometry in language that are most familiar to designers. The development of new OpenVSP features and capabilities has been extensively covered in publications and presentations over the years, but use case studies and best practises are frequently not documented. To illustrate the use of OpenVSP in the design process, this paper provides examples of advanced OpenVSP templates best practises.

Keywords: OpenVSP, Vehicle Sketchpad, aircraft, NACA 0010, lift, Drag.

Journal of Airline Operations and Aviation Management Volume 1 Issue 1
Received Date: 15 May 2022
Accepted Date: 10 June 2022
Published Date 25 July 2022

1. Introduction

Lift is produced by a propeller when fluid passes past it. The third law of motion of Newton or Bernoulli's principle, or maybe both, may be the cause of this lift. Due to the equal time argument, several academics have demonstrated that Bernoulli's principle is incorrect in certain circumstances [1].

Because both particles must arrive at the edge of the mark at the same time, the particles on the upper surface must travel farther than the particles on the lower surface. Because of this, Bernoulli's principle states that there is greater pressure at the bottom and less pressure at the top surface. Lift results from the pressure differential. The equal time argument is the formal name for this argument. Lift can be explained well using the equal time argument, however this is false [2]. The first mistake simulates how two particles cross surfaces of various lengths by starting from the same point and arriving at the rear edge at the same time. There are no two equally valid applications of the Bernoulli equation [5]. As a result, the equal-time argument theory cannot account for the lift produced by an aeroplane.

A closer examination of the curve reveals that the top of the bead will have higher pressure than the bottom, creating a centrifugal force that will drive the particles downward while the flow will continue to adhere to the impeller, a process known as the "Coanda effect" [6]. At the airfoil's base, the flow also curves. The bottom flow will curve more as a result of the curved bottom. Lift results from this flow [3]. The impeller will experience less pressure at the top, whereas the impeller will experience more pressure at the bottom. Lift is produced by this pressure differential. This is a fluid mechanics-based explanation [4].

The rotation of the aircraft along a lateral axis is referred to as pitch. It can be compared to the aircraft's "up and down" or "nodding" action[7]. The characteristic that most obviously separates operating an aeroplane in the air from operating any vehicle on Earth is altitude control.

Based on the integration of the scripting language in OpenVSP, user-defined components are functionally implemented in OpenVSP.. The scripting language AngelScript, which has a syntax similar to C/C++ and is intended to be incorporated into C++ programmes, was chosen for this job. Following the addition of a general-purpose scripting language to OpenVSP, programmers will naturally explore more applications for the capability.

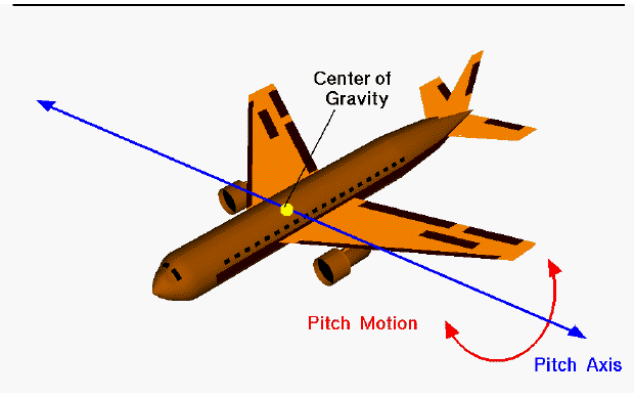

Figure 1: Pitch motion of an Aircraft[11]

2. DESIGN OF AN AIRCRAFT USING OPENVSP:

Visit the OpenVSP website to get the programme, which is mostly used for designing and analysing aeroplanes. In the workspace for aircraft design, more pieces are introduced for designing. Adding the wing is done in three stages as

indicated in the picture, now let's move on to the design. One side of the aeroplane wing is sufficient for design since the wing is symmetrical. The name is shown as major wing on the Gen tab. The default colour for the workspace is blue. The X, Y, and Z axes may be rotated and moved using the parameters on the Xform tab.Origin is set as (0,0,0) and symmetry is about xz axis, and it is given by default[8].

If this wing were attached to the parent and the parent was moved or rotated, the wing would not be affected since Attached to Parent is set to None for translation and rotation. As a few objects are often added as children, translation and rotation are applied farther down this hierarchy, changing tradition to comp as illustrated in the picture.

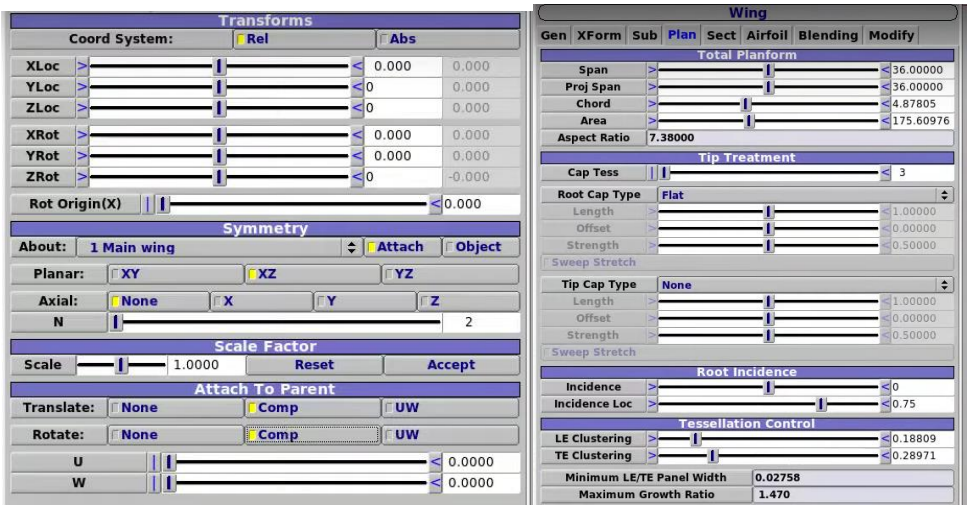

Figure 2: XForm and Plan in wing design

The plan shape is the next level; it has a 36-inch overall wingspan. The root and tip change concurrently when the chord is altered. The route expands faster than the tip since it is already larger while altering in ratio in relation to the existing chord. It is set to none for the tip caps type. The plane will spin by keeping the centre constant and by altering the incidence angle while maintaining the insurance position at 0.5. The tessellation control is really helpful for adding extra lines to the front edge, which is often where this curve needs more definition.

As seen in the image below, the wing is separated into three pieces in the wing portion. Both the root chord and the tip cord can be replaced. Changes to the Num U value will add or remove lines from that section, but they will remain minimal until the design is exported to workspace. As a result, the simulation programme for each of these lines will take longer to conduct calculations to determine what happens to the air as it flows off the trailing edge at that point. The image below depicts every setting in the section component; these settings were chosen for the design of the aeroplane wing.

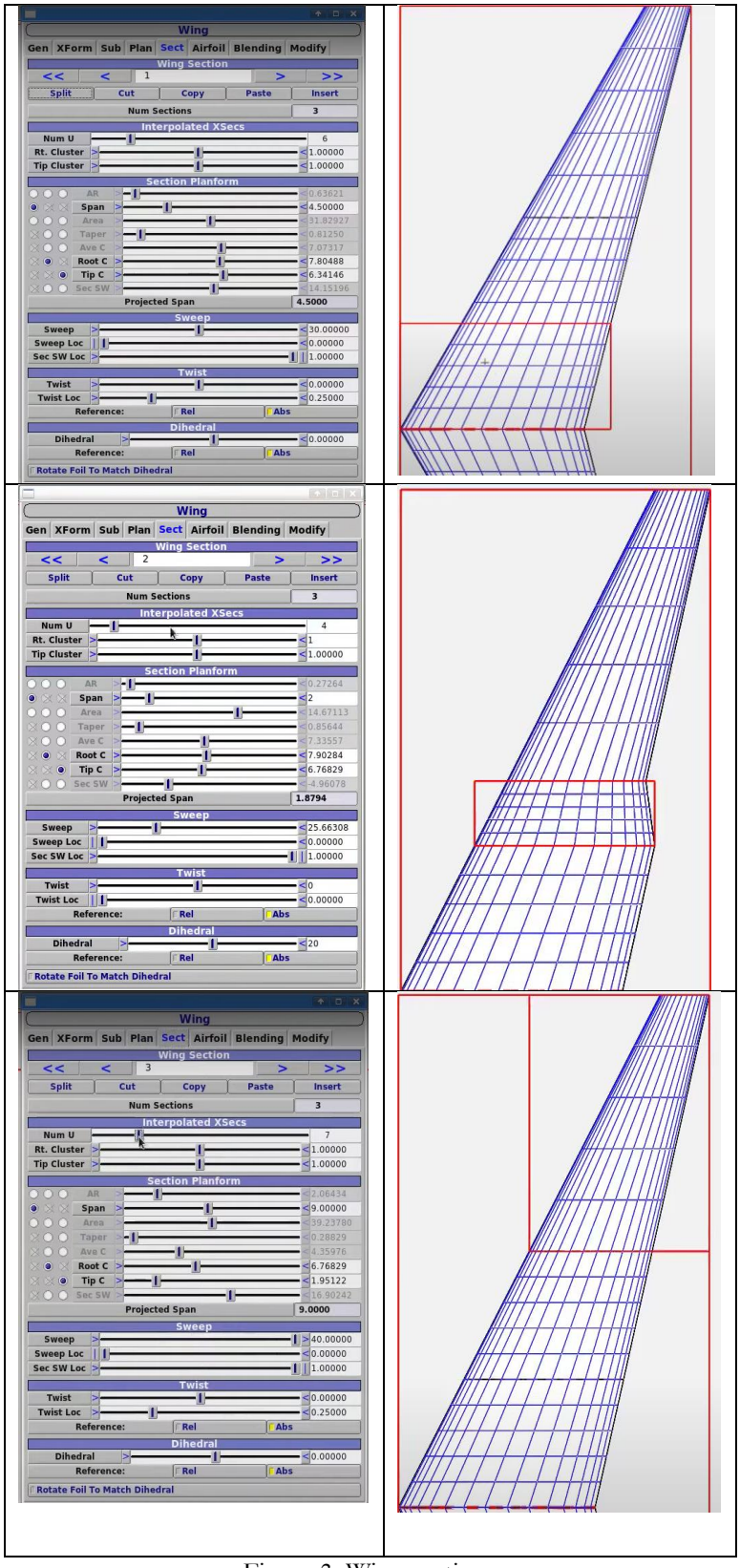

Figure 3: Wing sections

2.1. Airfoil:

By examining the tip airfoil, which will be number 3, we can. The default airfoil is NACA 0010, which indicates that the thickness to chord ratio is 10% and that camber may be increased or decreased in this airfoil. This is seen in the

image below. Additionally, there is a technique for designing airfoils that involves downloading coordinates from the UIUC database[9].

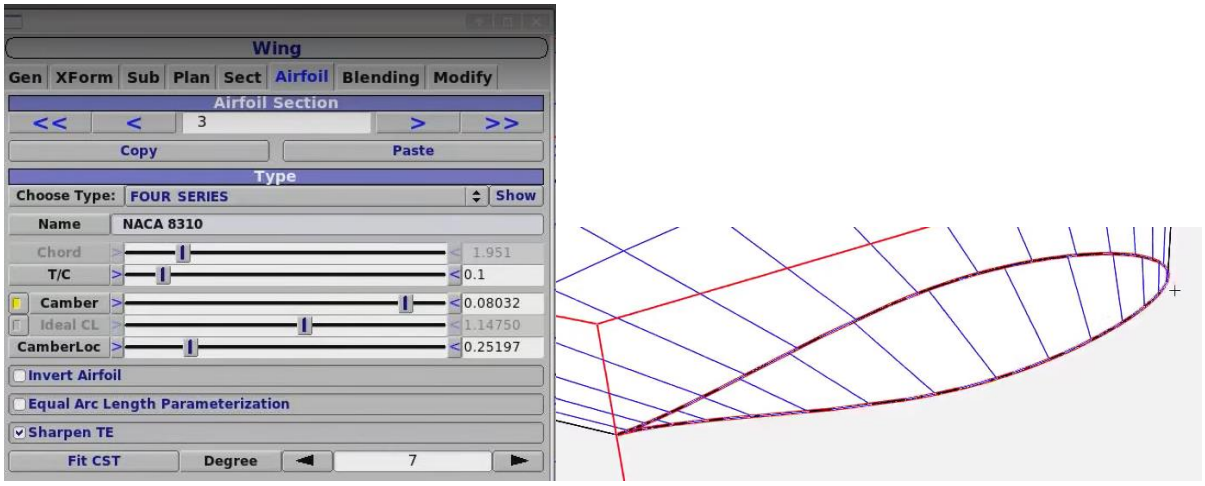

Figure 4: Airfoil Design

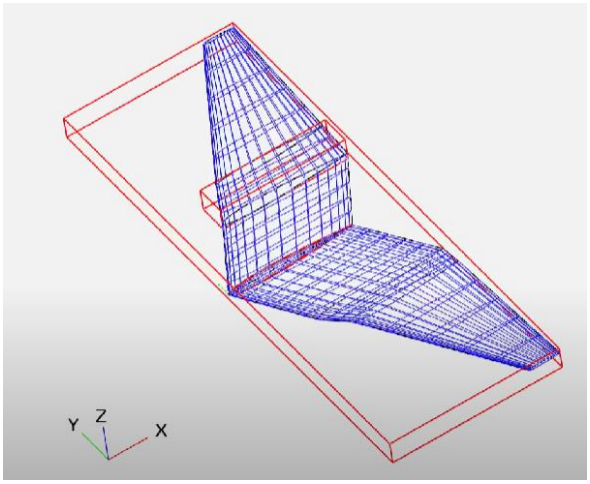

Figure 5: Wing design

2.2. Fuselage:

After determining the design parameters for the aircraft's wings and airfoils, the fuselage is now added to the Goem browser to produce the fuselage design. Position and rotation of the fuselage may be adjusted using the xform bar in the transform tab[10]. The cross section may first be clearly viewed by selecting the cross-section tab and selecting None to turn off the surface display. When seen from the front, there are 3 circles with elliptical cross sections. All of the alterations are made in the environment described below. The front part is changed from a point to a circle.

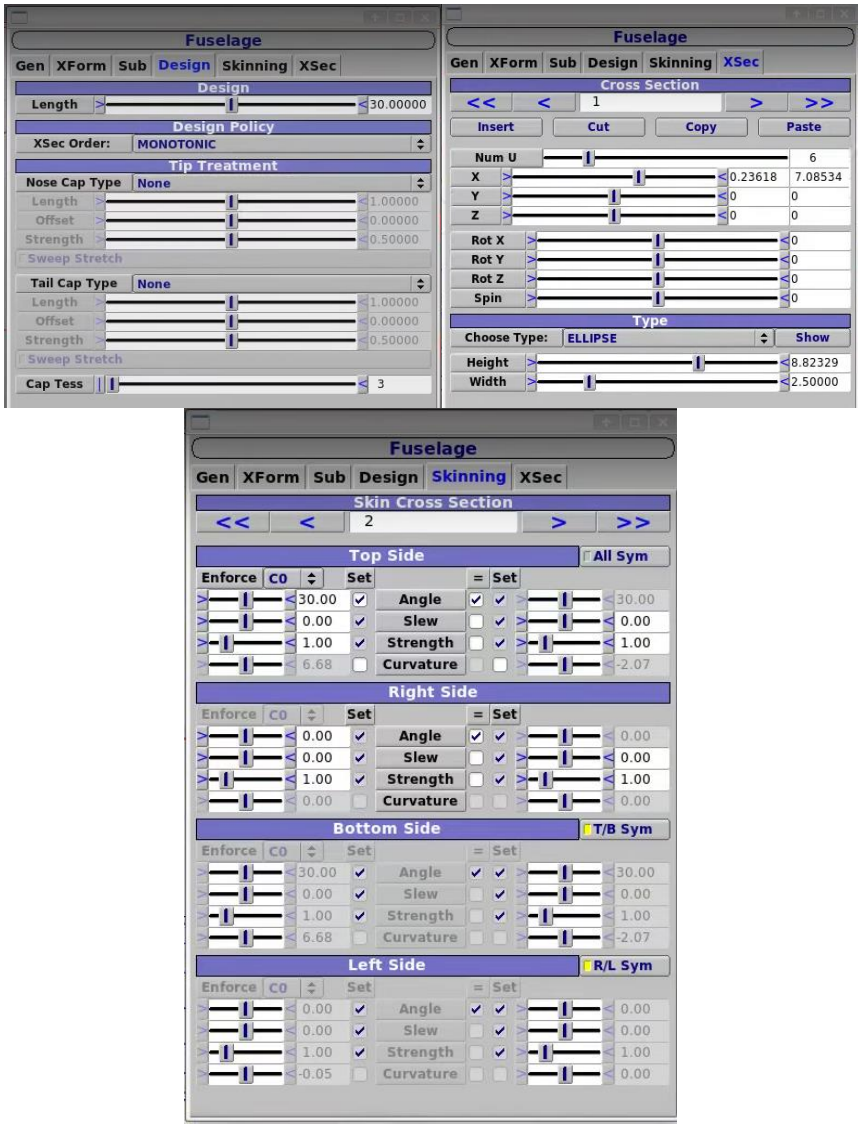

Figure 6: Fuselage design

3. RESULTS AND DISCUSSIONS:

Project Area Tab is used to measure the wing area. There is a target set that is presented, one that is not seen, and geometry set sets. Choose the suggested choice, and the z-axis should be projected. then begin the projection area's execution. A surface area of 40.9169 square centimetres was achieved. Prior to beginning any of these procedures, units should be chosen. Mesh is produced for the projection of the region.

Imagine that there is a piece of foam board in the direction of the airflow, which is moving from the left to the right. When the foam board is positioned at an angle from horizontal, lift and drag forces are measured. These numbers rely on a number of factors, including the size of the wing and the speed of the air flow. Graphs are used to compute the coefficients of lift and drag. The ratio of the coefficients of lift to the coefficient of drag, which were unitless numbers, is crucial. Weight and thrust, which exert forces downward and in the opposing direction of air flow, respectively, are the other two factors affecting the aircraft. Not only should we take these 4 forces into account, but also other factors like twisting and moment. The aeroplane will experience twisting force if the degree of inclination is large since there will be an anticlockwise moment. There will be a clockwise moment and twisting force when the angle

of inclination is negative. The key aspect is that when defining the direction of twisting force, the angle of attack in relation to the air flow is crucial. Coefficient of moment (CMy) is used to compute this, where y is the pitch axis.

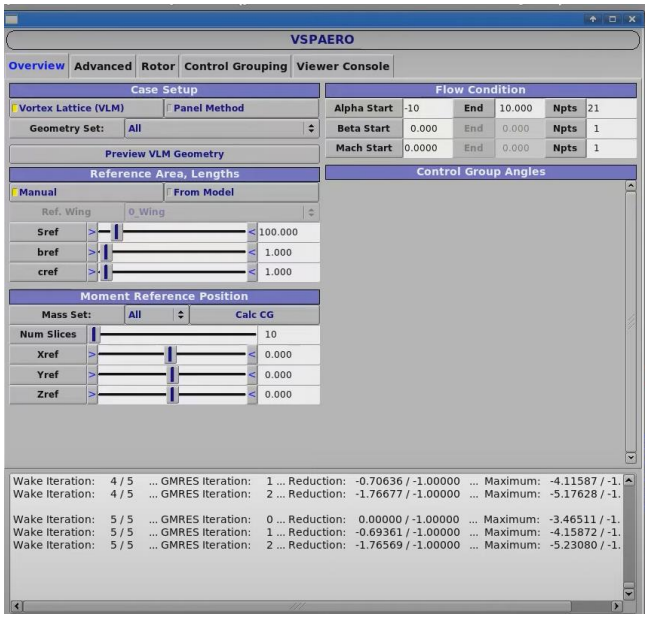

Figure 7: simulation

The forms of aircrafts are often complex in design and not simple. Since it is difficult to establish the centre of mass for each component and the process would be complicated, the coefficient 2 graphs, which are given below, may be used to estimate the angle of attack, coefficient of lift, and coefficient of drag, as well as any other equations. The results manager window displays the graphs below; there are three types of data available for choosing the specific graph. The span point y on the graph represents the distribution's centre. This graph displays the range of attack angles from -10 degrees to 10 degrees.

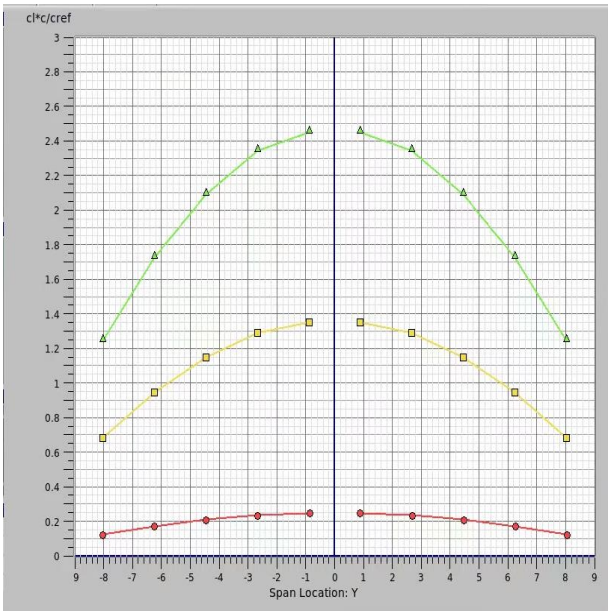

Figure 8: angle of attack vs cl

Unsteady pressures and steady pressures can be distinguished by launching the viewer. The maximum and lowest values of parameters may be found in the simulation tab's control surfaces, which display pressures, vorticity, triangulation, and trailing wakes. The number of sections along the wing constitutes the trailing wakes.

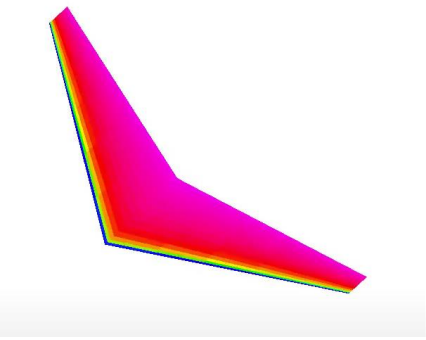

Figure 9(A): pressure

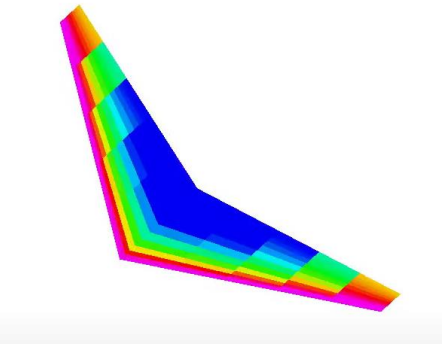

Figure 9(B): Vorticity

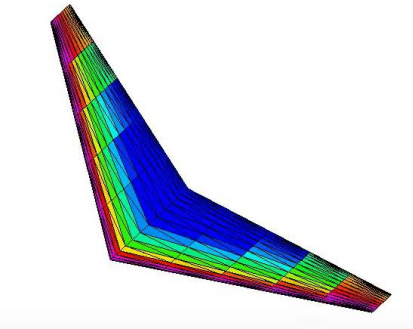

Figure 9(C): Triangulation

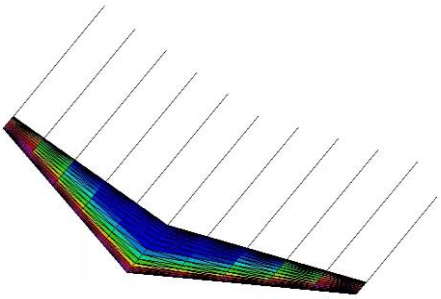

Figure 9(D): wakes

The graph is displayed below after altering the attack angle to 21 different angles. Additionally, the coefficient of moment graph may be identified. The graph between the angle of attack and the CMy is known as the coefficient of moment graph. Because the coefficient represents the pitching moment, if the value is greater than zero, the aircraft will tend to pitch upward. The plane is tilting downward if the value is less than zero.

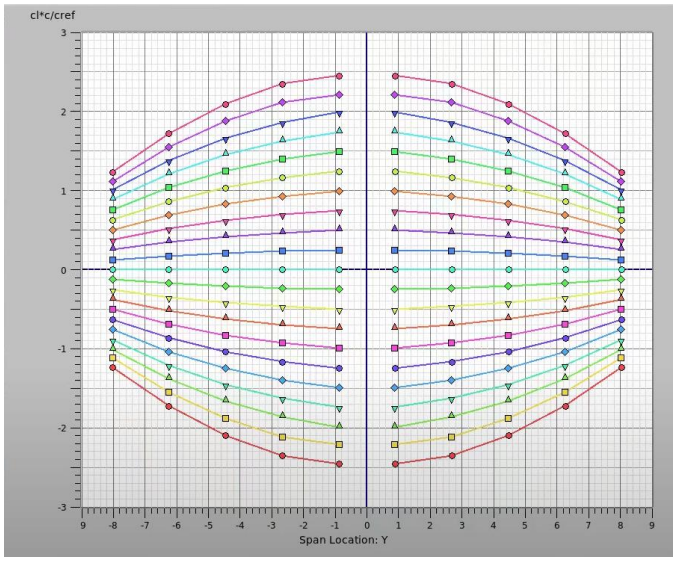

Figure 10: angle of attack vs cl

The pitching moment will turn negative if the angle of attack is excessive. Likewise, if the angle of attack is less than zero, the plane will remain neutral while the pitching moment turns positive. Figure 11 displays the graph if the centre of gravity is altered to 1.5. (B). The centre of gravity location has greater flexibility the steeper the slope.

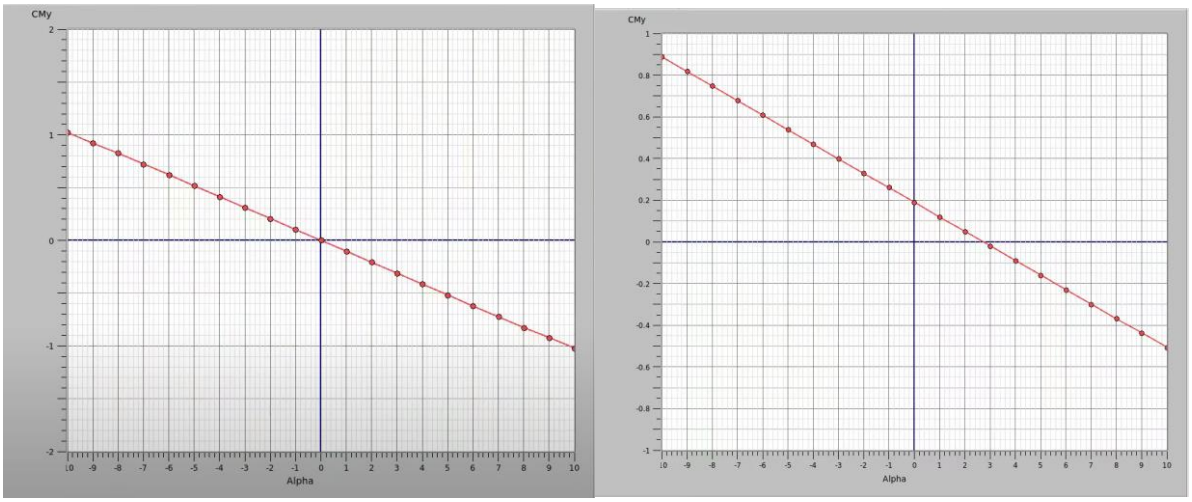

Figure 11(A) and 11(B): angle of attack vs CMy

Additionally displayed is the lift-to-drag ratio. The lift-to-drag force ratio and the angle of attack were shown on the graph. The centre of gravity is located at the tip in the first figure and 1.5 cm from the x axis in the following graph.

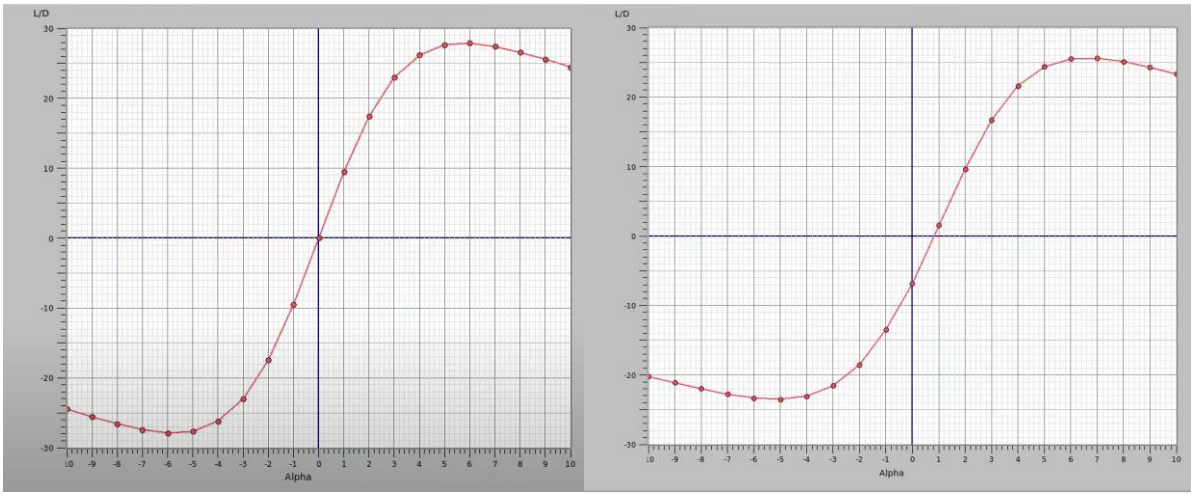

Figure 12: angle of attack vs L/D

4. CONCLUSION:

It was able to immediately compare Factor plot for a tunnel model of an aeroplane at angles of attack from -10° to +10° by gathering lift, drag, and pitch moment data with OpenVSP and translating them to the corresponding coefficients using proper calibration procedures. With increasing angle of attack, the experimental drag coefficient plot deviates less from the theoretical plot; potential explanations include the exclusion of higher longitudinal fins, thicker wings, insufficient biting resistance, and increased skin friction from turbulence. It is useful to place an item with a known coefficient of drag, such as a smooth sphere, in a wind tunnel on a fixed point in order to confirm that the inaccuracy is brought on by the circumstances on the model and not by erroneous calibration or data gathering. and contrast the measured and recorded drag coefficients. If the coefficients are the same, the model is where the erroneous nature originates. By calibrating the torque sensor numerous times on G, the torque coefficient may be evaluated.

References

[1] Jonathan Tompson, Kristofer Schlachter, Pablo Sprechmann, and Ken Perlin. Accelerating Eulerian Fluid Simulation With Convolutional Networks. arXiv, 2016.

[2] Julia Ling, Andrew Kurzawski, and Jeremy Templeton. Reynolds averaged turbulence modelling using deep neural networks with embedded invariance. Journal of Fluid Mechanics, 807:155–166, 2016.

[3] Brendan D. Tracey, Karthikeyan Duraisamy, and Juan J Alonso. A Machine Learning Strategy to Assist Turbulence Model Development. In 53rd AIAA Aerospace Sciences Meeting, pages 1–23, 2015.

[4] Andrea D. Beck, David G. Flad, and Claus-Dieter Munz. Deep Neural Networks for Data-Driven Turbulence Models. arXiv, 2018.

[5] Maziar Raissi, Paris Perdikaris, and George Em Karniadakis. Physics Informed Deep Learning (Part I): Data-driven Solutions of Nonlinear Partial Differential Equations. arXiv, pages 1–22, 2017.

[6] S. S. Bhat and R. N. Govardhan, "Stall flutter of NACA 0012 airfoil at low Reynolds numbers," Journal of Fluids and Structures, vol. 41, pp. 166-174, May 2013.

[7] N. Benard, J. Jolibois, and E. Moreau, "Lift and drag performances of an axisymmetric airfoil controlled by plasma actuator," Journal of Electrostatic, vol. 67, pp. 113-139, January 2009.

[8] Yousefi, Kianoosh and Reza Saleh. "Three-dimensional suction flow control and suction jet length optimization of NACA 0012 wing." Meccanica 50 (2015): 1481-1494.

[9] "UIUC Airfoil Data Site," UIUC Airfoil Data Site. https://mselig.ae.illinois.edu/ads/coord_database.html (accessed Jun. 11, 2022).

[10] "Turbulence Modeling Resource." https://turbmodels.larc.nasa.gov/naca0012_val.html (accessed Jun. 11, 2022).

[11] [4]"airplane pitch ." https://www.grc.nasa.gov/www/k-12/VirtualAero/BottleRocket/airplane/pitch.html (accessed Jun. 28, 2022).